On-Chip Contactless Four-Electrode Conductivity Detection for Capillary Electrophoresis Devices

**Frederic Laugere,*,† Rosanne M. Guijt,‡ Jeroen Bastemeijer,† Gert van der Steen,‡ Axel Berthold,§,||
Erik Baltussen,‡,⊥ Pascalina Sarro,§ Gijs W. K. van Dedem,‡ Michiel Vellekoop,# and Andre Bossche†**

*Electronic Instrumentation Laboratory—DIMES, Department of Microelectronics, Delft University of Technology, Delft,
The Netherlands, Section Analytical Biotechnology, Kluyver Laboratory for Biotechnology, Faculty of Applied Sciences,
Delft University of Technology, Delft, The Netherlands, ECTM, DIMES, Faculty of Electrical Engineering,
Delft University of Technology, Delft, The Netherlands, and Institute of Industrial Electronics and Material Science,
Vienna University of Technology, Vienna, Austria*

In this contribution, a capillary electrophoresis micro-device with an integrated on-chip contactless four-electrode conductivity detector is presented. A 6-cm-long, 70-μm-wide, and 20-μm-deep channel was etched in a glass substrate that was bonded to a second glass substrate in order to form a sealed channel. Four contactless electrodes (metal electrodes covered by 30-nm silicon carbide) were deposited and patterned on the second glass substrate for on-chip conductivity detection. Contactless conductivity detection was performed in either a two- or a four-electrode configuration. Experimental results confirmed the improved characteristics of the four-electrode configuration over the classical two-electrode detection setup. The four-electrode configuration allows for sensitive detection for varying carrier—electrolyte background conductivity without the need for adjustment of the measurement frequency. Reproducible electrophoretic separations of three inorganic cations (K^+, Na^+, Li^+) and six organic acids are presented. Detection as low as 5 μM for potassium was demonstrated.

In the development and optimization of miniaturized analytical systems, a delicate combination of science and technology originating from microelectronic device fabrication, electrical engineering, and analytical chemistry is essential. In this multi-disciplinary field, microtechnology experts combine the demands from analytical chemistry and electronic instrumentation in the design and fabrication of novel analytical devices.[1,2] Chemical analysis systems, such as high-performance liquid chromatogra-

phy (HPLC) or capillary electrophoresis (CE), always consist of the combination of a separation and a detection system.

For separation, CE or CE-based separation techniques are highly suitable for implementation on the microchip format. Electrokinetic control of fluid transport eliminates the need for external components such as pumps and valves. The separation efficiency is relatively independent of the separation path length and is, therefore, more compatible with miniaturization than, for instance, chromatographic techniques.

As far as detection is concerned, laser-induced fluorescence (LIF) is, at present, the most widely used detection technique in miniaturized analysis systems because of its high sensitivity. The drawbacks of LIF are its limited compatibility with miniaturization and on-chip integration and the requirement for labeling of most (bio) chemically relevant compounds. External devices such as the relatively large laser and the photodetector system strongly prohibit further miniaturization. The development of alternative detection methods compatible with miniaturization and full on-chip integration is highly desirable. Since electrode deposition is a well-established process in microfabrication, the implementation of detection techniques utilizing integrated electrodes has become an attractive approach. Successful coupling of conventional CE with potentiometry,[3] amperometry,[4,5] and conductometry[6−10] has been reported in the literature. In addition, both amperometric and potentiometric detection were also implemented in chip-based CE systems.[11−13] The primary advantage of amperometric and potentiometric detection over conductivity detection is the high selectivity induced by the electrochemical reactions that take place at the electrode surface. Only electrochemically active compounds

---

* Corresponding author: (tel) +31 (0) 15 278 6518; (fax) +31 (0) 15 278 5755; (e-mail) F.Laugere@its.tudelft.nl.
† Electronic Instrumentation Laboratory—DIMES, Department of Micro-electronics, Delft University of Technology.
‡ Section Analytical Biotechnology, Kluyver Laboratory for Biotechnology, Faculty of Applied Sciences, Delft University of Technology.
§ ECTM, DIMES, Faculty of Electrical Engineering, Delft University of Technology.
|| Present address: LAAS, Toulouse, France..
⊥ Present address: Notox B.V., Hambakenwetering 7, 5231, 's Hertogenbosch, The Netherlands.
Vienna University of Technology.
(1) Dolník, V.; Liu, S.; Jovanovich, S. *Electrophoresis* **2000**, *21*, 41−54.
(2) Bruin, G. J. M. *Electrophoresis* **2000**, *21*, 3931−3951.

(3) Kappes, T.; Hauser, P. C. *Anal. Chem.* **1998**, *70*, 2487−2492.
(4) Fang, X. M.; Gong, F. Y.; Fang, Y. Z. *Anal. Chem.* **1998**, *70*, 4030−4035.
(5) Gavin, P. F.; Ewing, A. G. *Anal. Chem.* **1997**, *69*, 3838−3845.
(6) Haber, C.; VanSaun, R. J.; Jones, W. R. *Anal. Chem.* **1998**, *70*, 2261−2267.
(7) Huang, X.; Zare, R. N. *Anal. Chem.* **1991**, *63*, 2193-2196.
(8) Fracasi da Silva, J. A.; do Lago, C. L. *Anal. Chem.* **1998**, *70*, 4339−4343.
(9) Mayrhofer, K.; Zemann, A. J.; Schnell, E.; Bonn, G. K. *Anal. Chem.* **1999**, *71*, 3828−3833.
(10) Zemann, A. J.; Schnell, E.; Volgger, D.; Bonn, G. K. *Anal. Chem.* **1998**, *70*, 563−567.
(11) Woolley, A. T.; Lao, K. Q.; Glazer, A. N.; Mathies, R. A. *Anal. Chem.* **1998**, *70*, 684−688.
(12) Rossier, J. S.; Roberts, M. A.; Ferrigno, R.; Girault, H. H. *Anal. Chem.* **1999**, *71*, 4294−4299.
(13) Wang, J.; Tian, B.; Sahlin, E. *Anal. Chem.* **1999**, *17*, 3901−3904.
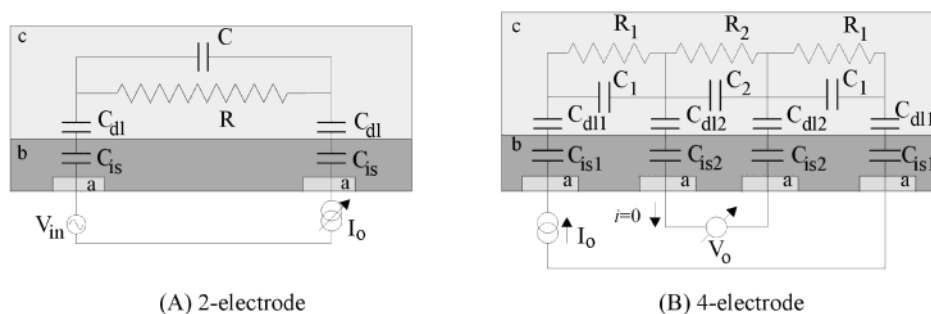
Figure 1. Electrical model of the contactless two- and four-electrode detector, including the respective measurement setup: (a) metal electrode; (b) insulating layer; (c) the conductive liquid; C_{is}, C_{dl}, C, and R are, respectively, the capacitance of the insulating layer, the double-layer capacitance, the capacitance of the liquid, and the resistance of the liquid.

can be detected using these methods, thereby eliminating interference with other compounds present in the sample. This selectivity, however, can also be turned into a disadvantage, since it strongly limits the applicability of the detection system. Additionally, the interference between the electrical separation field and the detection electrodes and associated electronics is a bottleneck for the realization of true on-column detection. Conductometry is a universal detection technique that has been applied to detection in CE in either the galvanic[6,7,14,15] or the contactless mode.[8-10,12] In both cases, a pair of electrodes is placed in the separation column for liquid impedance measurement. On one hand, conductivity detection has the advantage of being a universal detection method because separation and detection are based on charged analytes. On the other hand, conductivity detection is an "indirect" detection method for which the detection limit is highly limited by fluctuations of the background. Furthermore, separation and detection suffer from a conflicting requirement concerning the mobility of the separated ions and of the carrier electrolyte co-ion.[16] Recently, both galvanic[17-21] and contactless[22-25] conductivity detection were implemented on the microchip format. Galvanic detection was combined with isotachophoresis and with capillary zone electrophoresis. Various analytes were monitored such as metal ions, amino acids, proteins, and DNA fragments. The fabrication is rather easy: the platinum electrodes were either sputtered[17,18,21] or made from platinum wires sandwiched between

two pieces of polymer.[19,20] Contactless detection is preferred to galvanic detection for three reasons. First, the electronic circuitry is decoupled from the high-voltage applied for separation (no direct dc coupling between the electronics and the liquid in the channel). Second, the formation of gas bubbles at the metal electrodes is prevented, and third, electrochemical modification or degradation of the electrode surface is prevented, thereby allowing a wide variety of electrode materials. Lichtenberg et al.[23] presented a microchip where the detector is constructed with two opposite platinum electrodes placed close to the microchannel. The detection electrodes are isolated from the channel by a glass wall of ∼10 μm. Detection of potassium and lithium ions down to a concentration of 35 μM was reported. Recently, Pumera et al. presented a very easy-to-construct contactless conductivity detector consisting of two planar sensing aluminum film electrodes placed on the outside of a polymeric microchip.[24] A 125-μm-thick polymer (PMMA) sheet separates the electrodes and the channel. Detection limits down to 2.8 and 6.4 μM for potassium and chloride, respectively, were reported.

In this paper, we show that contactless liquid conductivity measurements achieved with a single pair of electrodes (two-electrode measurements) have a reduced sensitivity due to the presence of the insulating layer. In contrast with the two-electrode configuration, the use of four electrodes allows for sensitive detection with varying carrier–electrolyte conductivity without requiring adjustment of the measurement frequency. Glass microdevices with a miniaturized CE channel and an integrated contactless four-electrode conductivity detector were fabricated. The detector design allows for a comparison of the two- and four-electrode mode. On the basis of reproducible separations of a mixture of inorganic cations (K^+, Na^+, Li^+), the merits of the improved detection concept were demonstrated. Separations with concentrations down to 10 μM of these ions are reported, and a detection limit of 5 μM for potassium was obtained. Additionally, separation and detection of six organic acids extend the applicability of the new detection method.

CONTACTLESS TWO- AND FOUR-ELECTRODE LIQUID CONDUCTIVITY MEASUREMENT

To explain the preference for a four-electrode setup over a two-electrode setup (in the case of contactless conductivity measurements), the electrical representation of a conductivity cell (two- and four-electrode) is illustrated in Figure 1. The metal electrodes (a) are covered with an insulating layer (b). This insulating layer behaves electrically as a capacitor C_{is}, the value of which depends

(14) Zhao, H.; Dadoo, R.; Reay, R. J.; Kovacs, G. A.; Zare, R. N. *J. Chromatogr., A* **1998**, *813*, 205−208.

(15) Mo, J. Y.; Liu, W. F.; Mo, S. Y. *Anal. Commun.* **1998**, *35*, 365−367.

(16) Mikkers, F. E. P.; Everaerts, F. M.; Verheggen, Th. P. E. M. *J. Chromatogr.* **1979**, *169*, 1−10.

(17) Grass, B.; Neyer, A.; Jöhnck, M.; Siepe, D.; Eisenbeiss, F.; Weber, G.; Hergenröder, R. *Sens. Actuators, B* **2001**, *72*, 249−58.

(18) Masar, M.; Zuborova, M.; Bielckova, J.; Kaniansky, D.; Johnck, M.; Stanislawski, B. *J. Chromatogr., A* **2001**, *916*, 101−111.

(19) Prest, ?. ?.;; Baldock, S. J.; Fielden, P. R.; Brown, ?. ?. *Analyst* **2001**, *126*, 433−437.

(20) Galloway, M.; Stryjewski, W.; Henry, A.; Ford, S. M.; Llopis, S.; McCarley, R. L.; Soper, A. *Anal. Chem.* **2002**, *74*, 2407−2415.

(21) Guijt, R. M.; Baltussen, E.; van der Steen, G.; Schasfoort, R. B. M.; Schlautmann, S.; Billiet, H. A. H.; Frank, J.; van Dedem, G. W. K.; van den Berg, A. *Electrophoresis* **2001**, *22*, 235−241.

(22) Laugere, F.; Lubking, G. W.; Bastemeijer, J.; Vellekoop, M. J. *Proc. Transducers'01*, Munich, Germany, 2001; pp 1178−1182.

(23) Lichtenberg, J.; Verpoorte, E.; de Rooij, N. F. *Proc. Transducers'01*, Munich, Germany, 2001; pp 408−411.

(24) Pumera, M.; Wang, J.; Opekar, F.; Jelinek, I.; Feldman, J.; Lowe, H.; Hardt, S. *Anal. Chem.* **2002**, *74*, 1968−1971.

(25) Guijt, R. M.; Baltussen, E.; van der Steen, G.; Frank, J.; Billiet, H. A. H.; Laugere, F.; Vellekoop, M. J.; Berthold, A.; Sarro, P. M.; van Dedem, G. W. K. *Electrophoresis* **2001**, *22*, 2537−2541.
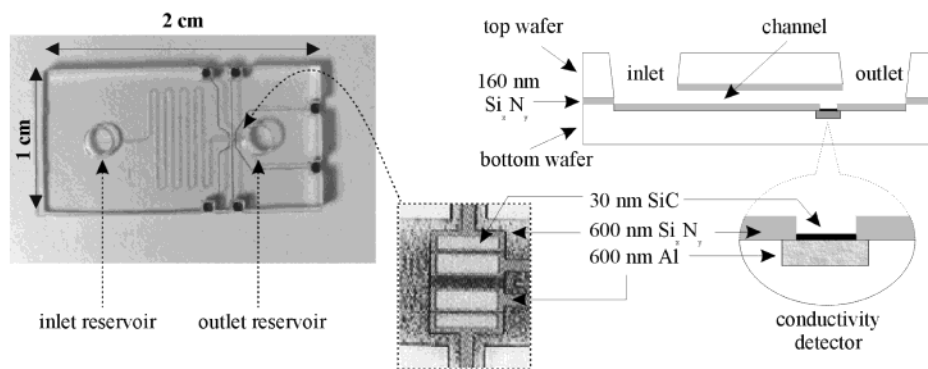
Figure 2. Top view (photograph) and cross section (schematic) of a miniaturized capillary electrophoresis device with contactless four-electrode conductivity detector. The photograph and the schematic inset show a closer view of the detector.

on its thickness and the area of the covered metal electrode. The double layer adds an extra capacitor C_{dl} in series with the insulating layer capacitor.[26] These two capacitors form the "electrode impedance". The conductive and dielectric contribution of the liquid (c) is represented by, respectively, a resistor R and a capacitor C (placed in parallel). Their values are linked to the spacing between the metal electrodes, the area of the electrodes, and the geometry of the channel. At low measurement frequencies, the dielectric contribution of the liquid is negligible.

In the two-electrode setup, an alternating voltage V_{in} is applied between the two electrodes and the resulting current I_0 is measured. Conventionally, liquid conductivity is retrieved from the measured liquid resistance, which is the result of the ratio V_{in}/I_0. However, the value of this ratio derives not only from the liquid resistance but also from the electrode impedance. Consequently, sensitivity and accuracy are lowered. This is even more so for a miniaturized detection cell where the electrode impedance is larger than the liquid resistance.

The four-electrode impedance setup allows circumventing the effect of the electrode impedance. A current I_0 with known amplitude is applied between the outer electrodes. A high input impedance differential amplifier is connected to the two inner electrodes. It does not draw a current because of its high input impedance. The measured differential voltage V_0 is, therefore, the voltage drop over the liquid resistance R_2. The liquid resistance R_2 (which is the reciprocal of the liquid conductivity) is retrieved from the ratio V_0/I_0 and does not include the electrode impedance. In this case, the observed sensitivity to changes in liquid conductivity is optimal.

EXPERIMENTAL SECTION

Device Fabrication. The CE microdevice used in this work was fabricated from two glass wafers (Corning No. 7740). The first wafer (top wafer) contains the channel and the inlet and outlet reservoirs. The second wafer (bottom wafer) contains the electrodes for conductivity detection (Figure 2). A detailed description of the complete fabrication process is given in ref 27.

The first step in processing the top wafer consists of wet etching reservoir holes (500 μm deep, 2.7-mm diameter) by means of HF-based solutions (aqueous solution of 70% H_3PO_4 and 5% HF at 70 °C). Once the reservoirs were created, the second step in the process was wet etching the channel using the same etching solution. The channel has a length of 6 cm, a depth of 20 μm, and a width of 70 μm at the separation part. At the detector part, the channel widens to 170 μm in order to provide adequate space for positioning the four electrodes. The third step was the deposition of a 160-nm-thick silicon nitride layer (PECVD layer) over the whole wafer, which enabled glass-to-glass anodic bonding.[28]

In the bottom wafer, a two-step trench (600 nm each) was etched by reactive ion etching. In the lower trench, aluminum electrodes and tracks were sputtered (at 20 °C). A 600-nm-thick silicon nitride (Si_xN_y) layer was deposited on top of the wafer (at 400 °C, using a Novellus PECVD reactor), thereby filling the second recess above the metal. The silicon nitride was isotropically etched in an inductive coupled plasma (ICP) etcher in order to planarize the wafer surface, enabling leakage-free bonding. For capacitively coupled conductivity detection, a very thin dielectric layer is required.[29] Therefore, the silicon nitride was removed at the position of the electrodes and replaced by a 30-nm-thick silicon carbide layer. The silicon carbide film was deposited at 400 °C, using a Novellus PECVD reactor. The insulating film has been kept very thin in order to obtain sufficient capacitive coupling to the liquid. All electrodes are 100 μm long, the two inner electrodes are 30 μm wide, and the two outer electrodes are 20 μm wide. The top and bottom wafers contained complementary alignment marks made out of recesses. These alignment marks were used for aligning the channel with the electrodes prior to bonding. After alignment, the wafers were anodically bonded at 400 °C and 1000 V for 1 h. This low-temperature bonding process was developed in order to achieve anodic bonding below the melting point of aluminum.[28] The bonding process resulted in a sealed electrophoresis channel with channel walls that are entirely covered with silicon nitride in order to obtain a uniform electroosmotic flow.

Experimental Setup. The microdevice was placed in a computer-controlled liquid-dispensing system operating with a dedicated injection procedure (IBIS Technologies BV, Enschede, The Netherlands). The inlet and outlet of the single-channel device were connected to 100-μL vials. Platinum wires, serving as high-

(26) Geddes, L. A.; Baker, L. E. *Principles of Applied Biomedical Instrumentation*, 3rd ed.; Wiley: New York, 1990; Chapter 9.

(27) Berthold, A. *Low-temperature wafer-to-wafer bonding for microchemical systems*; Deltech Uitgevers: Delft, 2001; Chapter 4 and 5.

(28) Berthold, A.; Nicola, L.; Sarro, P. M.; Vellekoop, M. J. *Sens. Actuators, A* **2000**, *82*, 224–228.

(29) Laugere, F.; Lubking, G. W.; Bastemeijer, J.; Vellekoop, M. J. *Sens. Actuators, A* **2001**, *92*, 109–114.
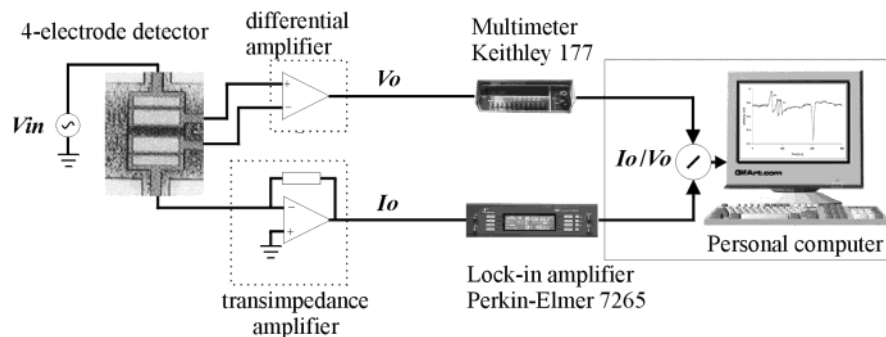
Figure 3. Measurement setup for the capacitive four-electrode liquid conductivity detection.

voltage electrodes, were positioned in the reservoirs and connected to a high-voltage supply assembled in-house. Injection was performed by means of a computer-controlled fluid-handling program. A drain in the inlet vial enabled fast removal of excess sample after injection. The injection procedure was typically as follows: empty the inlet and outlet reservoirs, fill the inlet with 70-μL sample, electrokinetic injection, empty the inlet reservoir via the drain port, fill subsequently the inlet and outlet reservoirs with 90 μL of buffer, and, finally, start the separation. The separation voltage remained switched on during the entire injection procedure, and the platinum electrodes remained in constant contact with the liquid (even when the vials were emptied, a small amount of liquid remained at the bottom of the vials). At the beginning of the injection procedure, the outlet reservoir was emptied in order to enable hydrostatic injection. However, the electrokinetic injection predominated over the hydrostatic injection due to the high flow resistance of the 6-cm-long channel. The entire injection procedure required $\sim$30 s.

A device holder compatible with the dispensing rack of the autosampler was fabricated in-house. The CE microdevice was glued onto a printed circuit board (PCB) and placed in the device holder. Thin bond wires were used to connect the connection pads of the glass microdevice to the tracks on the PCB. The low value of the insulating layer capacitor (10 pF) requires the readout electronics to be positioned as closely as possible to the detector, to minimize parasitic capacitance. Therefore, the readout electronic circuitry was implemented on another PCB and placed in the device holder, almost attached to the device.

The electronic connections for signal readout are depicted in Figure 3. A dedicated electronic interface was developed for the detector.[30] In a classical four-electrode setup,[31] an open-loop current source imposes a fixed current value between the outer electrodes. The parasitic capacitances of the leads, with values on the order of the insulating layer capacitance, induce unwanted current leakage. Therefore, it was decided to impose a voltage V_{in} (to one outer electrode) and to measure the resulting current I_o with a transimpedance amplifier (connected to the other outer electrode). Detailed information about transimpedance amplifier can be found in refs 30 and 32. The voltage imposed on the first outer electrode is not affected by the capacitance of the cable. Since the transimpedance amplifier has a low input impedance,

the parasitic capacitor on the second electrode does not have an influence either. In conclusion, this configuration is insensitive to parasitic capacitances within the operating frequency range (100 Hz$-$1 MHz).

The two inner electrodes were connected to a high input impedance (100 MΩ, 1 pF) differential voltage amplifier (V_o). An important factor in the selection of the differential voltage amplifier is the common mode rejection ratio (CMRR). The INA111 (Burr Brown Corp.) has a CMRR of 106 dB. A multimeter (Keithley 177 microvolt DMM, Keithley) and a lock-in amplifier (model SR830 DSP, Stanford Research Systems) respectively read the value of the differential voltage V_o (high-level signal) and I_o (low-level signal). Finally, the measured signals were sent to a PC through an acquisition card (KPCI 3108, Keithley Instruments), and the liquid conductivity value was retrieved from the real-time division of I_o/V_o, using the Labview software (National Instruments).

Reagents. Buffer solutions were prepared daily in MilliQ water (Millipore SA, Molsheim, France). 2-Morpholinoethanesulfonic acid (MES) was obtained from Sigma (St Louis, MO) and histidine (His) from Fluka (Buchs, Switzerland). All buffer solutions were filtered and degassed prior to use. Samples were diluted from 1 M stocks prior to analysis. NaCl, KCl, and LiCl were obtained from J.T. Baker (Deventer, The Netherlands).

The cleaning of the device was done once a day (before measuring). First the microchip was flushed with purified water for 5 min. Afterward, 2 M NaOH was used for reconditioning and cleaning of the capillary and the electrode surface (flushing during 5 min). Finally, the microchip was rinsed with purified water and manually filled with buffer before placement in the liquid-dispensing system.

RESULTS AND DISCUSSION

Comparison between the Two- and Four-Electrode Setup. The design of the contactless conductivity detector allowed comparison of the two- and four-electrode setup. Comparison was performed on the basis of the measured frequency response for varying buffer concentrations. The separation channel was filled with 0.2, 2, or 20 mM MES/His buffer at pH 6.0. The conductivities, measured at 20.4 °C with a commercial conductivity meter (Horiba ES14), were 8, 38, and 317 μS/cm, respectively. For each buffer concentration, the response (measured impedance equal to the ratio of V_o/I_o for the four-electrode setup and of V_{in}/I_o for the two-electrode setup) was measured in the frequency range of 100 Hz$-$1 MHz.

(30) Laugere, F.; Lubking, G. W.; Bastemeijer, J.; Vellekoop, M. J. *Sens. Actuators, B* **2001**, *83*, 104$-$108.
(31) Chroboczek, J. A.; Link, J. *J. Phys. Sci. Instrum.* **1985**, *18*, 568$-$570.
(32) Sedra, A. S.; Smith, K. C. *Microelectronic Circuits*, 4th ed.; Oxford University Press: New York, 1998; Chapter 2.
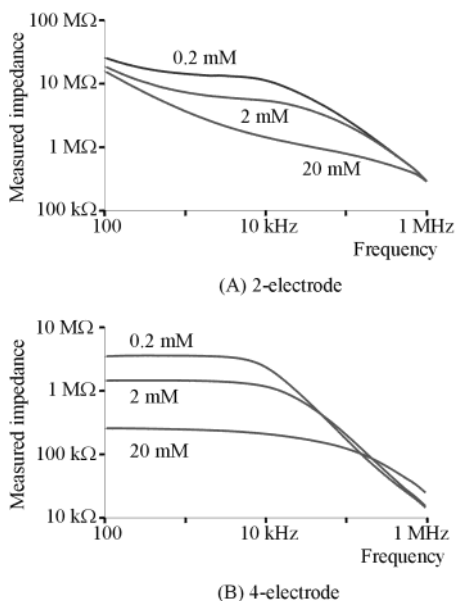
Figure 4. Measured impedance with a contactless two- and four-electrode setup (A and B, respectively). MES/His buffer (at pH 6) with concentration of 0.2, 2, and 20 mM (respective conductivities of 8, 38, and 317 μS/cm) was used.

The frequency response obtained with the two-electrode setup (Figure 4A) shows similar characteristics for each buffer conductivity, which can be divided into three frequency bands. At frequencies below 1 kHz, the insulating film acting as a capacitor (C_{is}) in series with the double-layer capacitance (C_{dl}) dominates the measured impedance. The double-layer capacitance is the only parameter sensitive to changes of conductivity,[26] resulting in a poor detection sensitivity in that frequency range. At frequencies above 100 kHz, stray capacitances C_{stray} (including capacitive coupling through the liquid) shortcut the liquid impedance, making the detector insensitive to conductivity changes. At medium frequencies (1−100 kHz), the measured impedance involves the liquid impedance and partly also the previously mentioned capacitances (C_{stray}, C_{is}, C_{dl}). In this frequency band, the detector is sensitive to changes in conductivity, but the accuracy, linearity, sensitivity, and dynamic range are determined by the values of C_{stray}, C_{is}, and C_{dl}. As expected from theory, there is a minor influence of C_{is} and C_{dl} on the frequency response of the four-electrode detector (Figure 4B). For frequencies up to 10 kHz, the detector response is linear with a constant and optimal sensitivity, whereas above 10 kHz, stray capacitances affect the detector response in the same way they affect the two-electrode setup. Using a 20 mM MES/His buffer, the usable range is extended to almost 100 kHz.

For conductivity detection in CE, the conductivity of the carrier electrolyte determines the baseline of the output signal. The output signal has to change with small variations in conductivity caused by analyte zones passing the detector. A capacitively coupled two-electrode configuration is suitable for this application, but as mentioned before, the detector response is highly dependent on the measurement frequency, which makes proper adjustment of that frequency a necessity. In addition, changing the conductivity of the carrier−electrolyte demands readjustment of the measurement frequency to obtain optimal sensitivity, linearity, accuracy, and dynamic range. This adjustment is not required for the four-
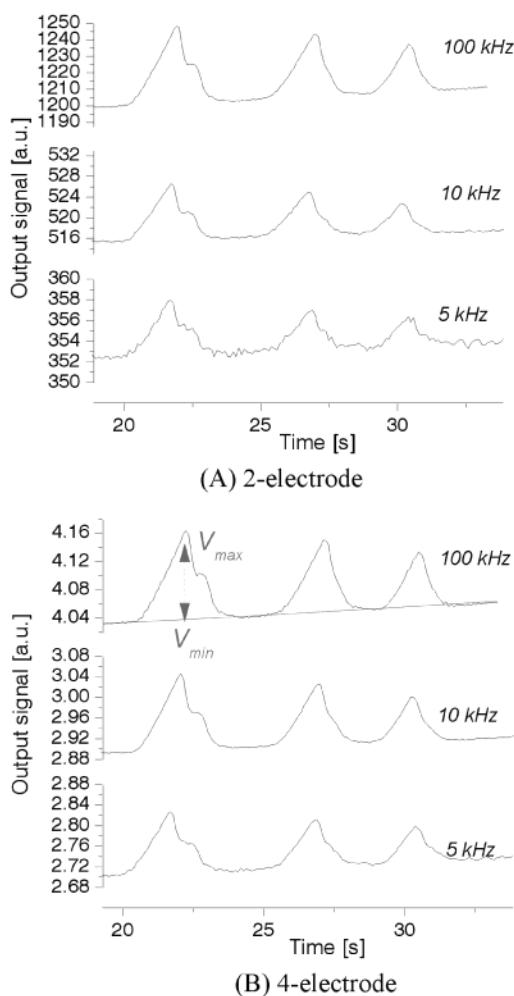
Figure 5. Separation of potassium, sodium, and lithium chloride (1 mM each) in a 20 mM MES/His buffer (pH 6.0). Conductivity detection was achieved with the contactless two-electrode setup (A) and four-electrode setup (B). The injection time was 1 s, the injection voltage was 483 V, the separation voltage was 1500 V (250 V/cm), and the measurement frequency was set to 5, 10, and 100 kHz.

electrode configuration, where detection performance (in terms of sensitivity) is similar for each buffer concentration when measurements were at frequencies below 10 kHz.

Separation of Inorganic Ions. Electrophoretic separations were performed in 20 mM MES/His buffer at pH 6.0. The injected sample consisted of a 1 mM mixture of potassium, lithium, and sodium chloride in MilliQ water. The injection time (time the sample remained in the sample reservoir for electrokinetic injection) was 1 s, and the applied injection voltage was 483 V. For separation, the voltage applied to the channel was increased to 1500 V. The measurement frequency was set to 5, 10, and 100 kHz. The resulting electropherograms obtained with the four-electrode setup are shown in Figure 5B. The three peaks corresponding to K^+, Na^+, and Li^+ are clearly resolved with complete separation in just under 33 s. The same measurements were performed with the two-electrode setup (Figure 5A). The peak shapes obtained for K^+, Na^+, and Li^+ are analogous to the ones obtained previously using the four-electrode setup. The distortion observed on the potassium peak is a result of the injection: during the injection sequence, sample and buffer were drawn in and out of the sample reservoir while a voltage remained

applied to the separation channel. After electrokinetic injection, the sample cannot be replaced instantaneously with buffer and an excess of sample is injected (observed as the distortion). To prevent that problem, the voltage applied to the separation channel could be switched off during dispensing and removal of sample and buffer in the sample reservoir. An improved shape of the peak was observed. However, the amount of sample injected considerably decreased, resulting in a poor detection limit. For that reason, we decided to keep the voltage switched on during the injection sequence.

The obtained electropherograms are in accordance with the frequency responses shown in Figure 4A and B. For comparison, one should keep in mind that liquid impedance is inversely proportional to liquid conductivity. The two-electrode response shows that the magnitude of the baseline, which is linked to the conductivity of the buffer, changes with respect to the measurement frequency (353, 516, and 1200 arbitrary units at 5, 10, and 100 kHz, respectively). This is in agreement with the frequency response obtained in Figure 4A where the measured impedance (reciprocal of the conductivity) decreases with respect to the measurement frequency. The four-electrode response shows a behavior that is, as well, consistent with the measured frequency responses of Figure 4B. The baseline value slightly increases for frequencies below 10 kHz (2.68 and 2.80 arbitrary units at 5 and 10 kHz, respectively), and above 10 kHz, it distinctly increases (4.04 au at 100 kHz) due to the effect of parasitic capacitances.

The sensitivity of a conductivity cell, as it is usually considered, is the ratio of the magnitude of the output signal and the magnitude of the conductivity (expressed in volt/siemens). It takes into account the input signal amplitude and the various amplifications of the measured signal. This is an absolute sensitivity, which does not reflect the intrinsic sensitivity of the detection cell. The sensitivity coefficient S is more suitable for characterization of the conductivity cell.[33] It is defined as the percent change in output signal due to a 1% increase in concentration. It is numerically estimated as

$$S = 100(V_{max} - V_{min})/(V_{min})$$

where V_{max} and V_{min} are the magnitude of the output signal corresponding to the baseline and to the peak height, respectively (see illustration in Figure 5A on the potassium peak). From the previous electropherograms, the sensitivity coefficient of the two- and four-electrode setup response for the three ions was calculated.

In Figure 6, the profile of the sensitivity coefficient versus the measurement frequency in the frequency range (1−200 kHz) is plotted. For each measurement setup, the profile is similar for the three ions. The plot for the two-electrode shows a linear increase of the sensitivity, between 2 and 100 kHz (at logarithmic scale), which is inversely proportional to the decrease of the "electrode impedance". The sensitivity coefficient reaches an optimal value at ∼100 kHz with a value equal to 3.84% for potassium. The two previous observations are in agreement with the measured frequency response shown in Figure 4A (with 20
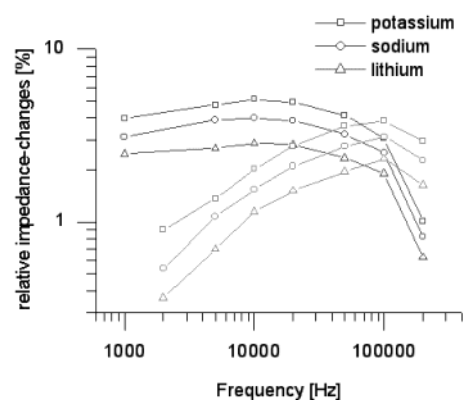
(33) Jay, F.; Goetz, J. A. *IEEE Standard Dictionary of Electrical and Electronics Terms*, 3rd ed.; The Institute of Electrical and Electronics Engineers, Inc.: New York, 1984.

Figure 6. Sensitivity versus measurement frequency with contactless two- and four-electrode setup. The bottom set of curves (gray lines) concerns the two-electrode response. The top set of curves (black lines) concerns the four-electrode response.
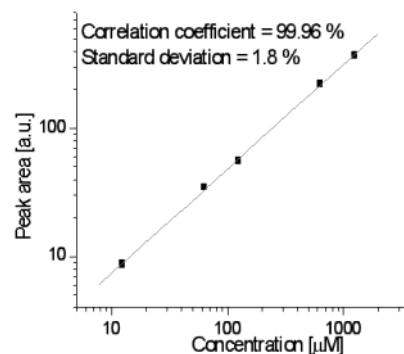

Figure 7. Peak area versus sample concentration using contactless four-electrode conductivity detection. The sample consisted of potassium at concentrations ranging from 12.5 μM to 1.25 mM. The injection time was 1 s, the injection voltage was 483 V, the separation voltage was 1500 V (250 V/cm), and the measurement frequency was set to 10 kHz

mM MES/His). Measurements below 2 kHz were not possible because the signal was below the noise level. As expected from theory, the sensitivity coefficient with the four-electrode setup is increased and that in an extended frequency range when compared to the two-electrode setup. In Figure 6, the sensitivity is always higher for the four-electrode detector in the frequency range 1−70 kHz. At high frequencies, the sensitivity coefficient drops due to the influence of the parasitic capacitances. The optimal sensitivity coefficient (5.12% for potassium) is obtained at a measurement frequency of 10 kHz. A slight but constant decrease of the sensitivity coefficient is observed below 10 kHz, which is not consistent with the theory. We do not yet have an explanation for that decrease.

The linearity of the detector was demonstrated by injecting only potassium at concentrations ranging from 1.25 mM to 12.5 μM. The 20 mM MES/His (pH 6) was used as background electrolyte. The injection was done at 483 V and the separation at 1500 V. Two measurement cycles were performed for each concentration. The measurement frequency was set to 10 kHz, and the peak area was extracted from each electropherogram. The results are shown in Figure 7, where the linearity of the detector is demonstrated through a correlation coefficient for the linear fit equal to 99.96%.

The reproducibility of the detector response has been tested over 21 consecutive runs (3 h in total). For each run, a sample
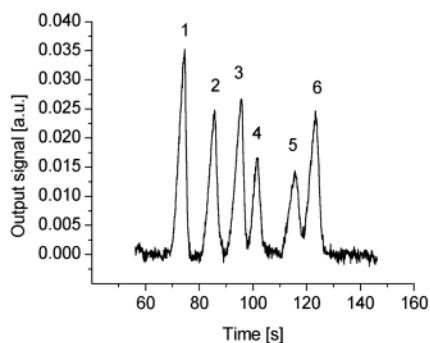
Figure 8. Separation of a mixture of fumaric (1), citric (2), succinic (3), pyruvic (4), acetic (5), and lactic acids (6) (1 mM each). A 20 mM MES/His (pH 5.8) solution with 0.2 mM TTAB for reversing the electroosmotic flows was used as the carrier electrolyte. Injection was performed by ramping the voltage from 0 to −1000 V and back up to 0 V (total time is 800 ms). The applied separation voltage was 1000 V (167 V/cm).

containing 1 mM potassium, sodium, and lithium was injected. A 20 mM MES/His (pH 6) solution was used as background electrolyte. The injection was done at 483 V and the separation at 1500 V. The measurement frequency was set to 10 kHz, and the peak area was extracted for all runs. Relative standard deviations of 1.39, 0.92, and 0.72% were obtained for, respectively, potassium, sodium, and lithium.

Electrophoretic separations were performed at concentrations down to 10 μM for each ion and at the optimal measurement frequency (10 kHz). Detection limits of 5 μM for potassium, 15 μM for lithium, and 10 μM for sodium were obtained (detection limit defined as three times the baseline noise-level). The signal-to-noise-ratio (SNR) was the same for both detectors when measurements were at the optimal frequency (10 and 100 kHz for the four-electrode and two-electrode setup, respectively). However, the SNR decreased drastically for the two-electrode setup when measurements were at frequencies different from the optimal one. Below 2 kHz, detection was even not possible anymore. As far as the four-electrode detector was concerned, the SNR also decreased when measurements were not taken at the optimal frequency. However, thanks to a higher sensitivity, detection at frequencies as low as 600 Hz was possible.

The achieved detection limit is slightly higher than the values reported in ref 24 (2.8 and 6.4 μM for potassium and lithium, respectively). However, two major differences between our device and the one described in ref 24 determine the achievable detection limit. First, the presence of abrupt turns in the channel design is a source of zone dispersion.[34] Second, the single-channel geometry does not allow injection of a short, well-defined sample plug. Improvements in peak shape and detection limit are expected by using cross-injection geometry in combination with a straight channel.

Separation of Peptides and Organic Acids. In an earlier publication,[21] we showed the separation of a mixture of two

(34) Culbertson, C. T.; Jacobson, S. C.; Ramsey, J. M. *Anal. Chem.* **1998**, *70*, 3781−3789.

peptides (1 mM each) performed in a 50 mM phosphate buffer at pH 2.5. The injection time was 3 s, while the voltage was kept at 300 V for injection and separation.

We also performed separations of six organic acids, namely, fumaric, citric, succinic, pyruvic, acetic, and lactic acid (Figure 8). The buffer was 20 mM MES/His at pH 5.8 to which 0.2 mM of TTAB was added to reverse the electroosmotic flow. A negative power supply (assembled in-house) was used for injection and separation. The sample was injected electrokinetically by applying a voltage when the sample was present in the sample reservoirs. In contrast with the measurements described before, the high-voltage source was switched off during liquid-handling steps in the reservoirs. If not, peaks were distorted and became too wide to allow baseline separation (see peak distortion in Figure 5A and B). During injection, the voltage is ramped down from 0 to −1000 V and ramped up to 0 V in 800 ms (total time). Longer injection time overloaded the injected sample and resulted in overlapping of the peaks. The separation was done at −1000 V (167 V/cm). The direct consequence of the modified injection method is a relatively poor detection limit when compared to inorganic ions: a detection limit of 100 μM is deduced on the basis of the noise level.

CONCLUSION

This paper clearly demonstrates the benefits of the use of four electrodes for contactless conductivity detection in miniaturized CE devices. The influence of the electrode impedance (double-layer capacitance and insulating layer capacitance) on the response is minimized. Consequently, at frequencies below 10 kHz, the detector response (sensitivity, linearity, accuracy) is almost independent of the measurement frequency and of the conductivity of the carrier electrolyte.

The conductivity detection method was evaluated in a CE microdevice in which electrophoretic separations of a mixture of inorganic cations (potassium, sodium, lithium) were performed. On-column detection with a separation field of up to 250 V/cm could be achieved. The three peaks could be clearly detected with considerable improvement in sensitivity compared to the classical two-electrode setup. Detection limits ranging from 15 down to 5 μM (depending on the ion) were obtained.

Finally, separation of six organic acids was demonstrated, extending the applicability of the contactless four-electrode detector.